



# Neutrinos and their interactions

M. Sajjad Athar<sup>a</sup> and S. K. Singh

Department of Physics, Aligarh Muslim University, Aligarh 202002, India

Published online 11 November 2021

© The Author(s), under exclusive licence to EDP Sciences, Springer-Verlag GmbH Germany, part of Springer Nature 2021

**Abstract** We present a short overview of the importance of the study of neutrino interactions in the intermediate- and high-energy region, with an introduction to the neutrinos and a very brief description of the collection of invited articles.

The story of neutrino physics has been an amazing one, starting in 1930 with the hypothesis of Pauli’s “neutron” [1], assumed to be a massless, chargeless fermion of spin  $\frac{1}{2}$ , in order to explain the two outstanding problems of that time associated with the conservation laws: the conservation of energy and the conservation of angular momentum. This hypothesis was given a solid foundation in 1933 with the theory of beta decay [2] propounded by Fermi, who rechristened Pauli’s “neutron” to “neutrino” and argued that the four-point interaction vertex in a beta decay is vectorial in nature. Later, with the observations of parity violation in beta decay [3] and the observation of neutrinos to be left-handed particles [4], it was established that the weak interaction vertex was of a V-A (vector-axial vector) nature, and a theory of neutrino interaction with matter was formulated using chiral ( $\gamma_5$ ) invariance assuming neutrinos to be massless [5–9]. To avoid ultraviolet catastrophe in  $\nu_e - e$  scattering, it was assumed that the interaction is mediated by a heavy boson. In 1956, an electron-type neutrino (or rather an antineutrino  $\bar{\nu}_e$ ) was detected at the Savannah River reactor [10, 11]. Later it was observed that there are three different flavors of neutrinos, namely electron neutrino ( $\nu_e$ ), muon neutrino ( $\nu_\mu$ ), and tauon neutrino ( $\nu_\tau$ ), which are characterized by their own lepton quantum number  $L_e$ ,  $L_\mu$ , and  $L_\tau$ , and these are conserved separately in the weak interaction. In the Standard Model (SM) of particle physics [12–14] currently known to best describe the properties of the fundamental particles and their interactions, there are three generations of lepton flavors, each placed in a weak isospin doublet where, corresponding to each charged lepton, i.e.  $e^-$ ,  $\mu^-$ , and  $\tau^-$ , there is a massless neutrino of the same lepton number, i.e.  $\nu_e$ ,  $\nu_\mu$ , and  $\nu_\tau$ . The existence of three flavors of neutrinos was experimentally established in 1989 when the large electron-positron collider (LEP) confirmed the presence of three active neutrinos [15]. The interactions

of these neutrinos with matter are described by the SM gauge bosons, i.e.  $W^+$ ,  $W^-$ , and  $Z^0$ . The absolute masses of neutrinos are not known, and there are upper experimental limits on them obtained from the end point spectrum of beta decay for  $\nu_e$ , pion decay for  $\nu_\mu$ , and tauon decay for  $\nu_\tau$ , as well as from other indirect methods.

The evolution in our understanding of the physics of neutrinos is full of surprises, as they continue to challenge our expectations regarding the validity of certain symmetry principles and conservation laws in particle physics. Today, we know that neutrinos are the most abundant particles in the universe after photons, but are the least understood, due to their weakly interacting nature, although they play an important role not only in particle and nuclear physics, but also in cosmology and astrophysics. There are natural sources of neutrinos such as those produced during nuclear fusion inside a star’s core, supernova bursts, decay of secondary cosmic ray particles in the earth’s atmosphere, and geoneutrinos produced in the earth’s core, as well as artificial sources of neutrinos like those produced from nuclear reactors and particle accelerators. Many of these neutrino sources are being used to explore the properties of neutrinos and their interactions with matter. These neutrinos are also helpful in understanding the various astrophysical phenomena with respect to the sun’s core, composition of the earth’s core, and time and place of supernova explosion [16].

The observations of the solar neutrino anomaly and the atmospheric neutrino puzzle are generally understood on the basis of neutrino flavor oscillation, a quantum mechanical effect which implies that at least two of these neutrinos have tiny masses. The observation of the phenomenon of neutrino oscillation therefore requires new physics beyond the Standard Model (BSM). Neutrino oscillation has also been observed in both accelerator and reactor neutrino experiments. The three neutrino flavor states  $\nu_e$ ,  $\nu_\mu$ , and  $\nu_\tau$  of the SM are considered to be a mixture of the

<sup>a</sup> e-mail: [sajathar@gmail.com](mailto:sajathar@gmail.com) (corresponding author)

three mass eigenstates  $m_1$ ,  $m_2$ , and  $m_3$ . The mixing is described in terms of the Pontecorvo-Maki-Nakagawa-Sakata (PMNS) matrix [17, 18], which is most popularly parameterized in terms of the three mixing angles  $\theta_{12}$ ,  $\theta_{13}$ , and  $\theta_{23}$ , and a phase  $\delta$ , better known as  $\delta_{CP}$ , as it can be used to describe charge conjugation-parity (CP) violation. Some of these oscillation parameters have been determined in solar, reactor ( $\theta_{12}$ ), accelerator ( $\theta_{13}$ ), and atmospheric ( $\theta_{23}$ ) neutrino experiments. One important determination which has yet to be made is whether the neutrinos follow normal mass hierarchy ( $m_1 < m_2 < m_3$ ) or inverted mass hierarchy ( $m_3 < m_1 < m_2$ ). This is because the neutrino oscillation experiments can determine only the square of the mass differences  $\Delta m_{21}^2$  (sensitive solar and reactor sources) and the absolute value of  $|\Delta m_{31}^2|$  (sensitive to reactor, accelerator, and atmospheric), and the sign of  $\Delta m_{31}^2$  is required to settle the mass hierarchy problem. There has recently been some information on  $\delta_{CP}$ , but it is very limited. To understand the properties of neutrinos and to determine the various parameters of the PMNS matrix and CP violation phase  $\delta_{CP}$ , as well as the mass hierarchy in neutrino mass eigenstates, several experiments in the low energies (corresponding to reactor, solar, and supernova neutrinos) and medium energies (corresponding to accelerator and atmospheric neutrinos) are being performed.

In the region of very low energy relevant for the reactor and solar neutrinos, the exclusive transitions to the ground state or a few low excited states in the final nucleus are accessible. In the medium- and high-energy regions, accelerator experiments including Mini Booster Neutrino Experiment (MiniBooNE), Tokai to Kamioka (T2K), SciBar Booster Neutrino Experiment (SciBooNE), CERN neutrinos to Gran Sasso (CNGS), The Oscillation Project with Emulsion tRacking Apparatus (OPERA), and NuMI Off-axis  $\nu_e$  Appearance (NOvA), as well as atmospheric neutrino experiments such as SuperKamiokande and IceCube, have (anti)neutrinos in the energy range sufficient to excite many nuclear states; the energies are sufficient to create new particles and can induce various inclusive processes of quasielastic, inelastic (e.g.  $1\pi$ ,  $1\eta$ ,  $1K$ ,  $YK$  ( $Y = \Lambda, \Sigma$ ) production), and deep inelastic scattering processes, given by [16]:

$$\begin{aligned} \nu_l (\bar{\nu}_l) + N &\longrightarrow l^- (l^+) + N', && \text{(quasielastic)} \\ \bar{\nu}_l + N &\longrightarrow l^+ + Y, && \text{quasielastichyperon(Y)production} \\ \nu_l (\bar{\nu}_l) + N &\longrightarrow l^- (l^+) + N' + X, && \text{(inelastic), } X = \pi, K, \eta, \\ \nu_l (\bar{\nu}_l) + N &\longrightarrow l^- (l^+) + Y + K(\bar{K}), && \text{(inelastic Associated particle} \\ &&& \text{production)} \\ \nu_l (\bar{\nu}_l) + N &\longrightarrow l^- (l^+) + \text{jet of hadrons (deep} && \\ &&& \text{inelastic scattering), where} \\ &&& N, N' = n \text{ or } p. \end{aligned}$$

This volume is focused on the interaction of the intermediate- and high-energy neutrinos in the region

of a few giga-electron volts (GeV). The inclusive cross sections in the quasielastic region are analyzed in terms of the weak form factors of the nucleon, and the cross sections in the inelastic scattering corresponding to the excitations of various nucleon resonances lying in the first or higher resonance regions are described in terms of the transition form factors corresponding to the nucleon resonance transition. On the other hand, if the energy transfer ( $\nu$ ) and the four-momentum transfer squared ( $Q^2$ ) are large, the inclusive cross sections are expressed in terms of the structure functions corresponding to the deep inelastic scattering process from the quarks and gluons in the nucleon. In the intermediate-energy region corresponding to the transition between resonance excitations and deep inelastic scattering, we have yet to find a method best suited to describe the inclusive charged lepton or (anti)neutrino scattering processes. The use of the kinematic cuts in the  $Q^2 - \nu$  plane (Fig. 1) may enable us to understand the elastic scattering ( $W = M$ ), inelastic scattering ( $M \leq W \leq 2$  GeV), deep inelastic scattering ( $Q^2 > 1\text{GeV}^2$ ,  $W > 2$  GeV), and soft deep inelastic scattering, ( $Q^2 < 1$  GeV<sup>2</sup>,  $W > 2$  GeV) regions.

In the quasielastic region, for the scattering of (anti)neutrinos with the nucleons, the identity of the nucleons remains intact except for the  $\Delta S = 1$  reaction, where a nucleon is converted into a hyperon (in the case of  $\bar{\nu}$  only). In the inelastic region, the scattering leads to the excitation of various resonances. The resonance excitation of the nucleon includes isospin  $I = \frac{1}{2}$  resonances such as  $N^*(1440)$ ,  $N^*(1520)$ , and  $N^*(1535)$ , and isospin  $I = \frac{3}{2}$  resonances such as  $\Delta(1232)$ ,  $\Delta^*(1600)$ , and  $\Delta^*(1700)$ , together with a non-resonant continuum. The decays of these resonances lead predominantly to a single pion, i.e.  $\pi N$  state, and also to other final states including  $\gamma N$ ,  $\eta N$ ,  $KY$ ,  $\pi\pi N$ , and  $\rho N$ . The shallow inelastic region (SIS) covers resonance excitation on the nucleon that, together with a non-resonant continuum, leads predominantly to the abovementioned final states. In Fig. 1, we show the importance of the different kinematic regions relevant for the quasielastic, inelastic, and deep inelastic scattering corresponding to the two neutrino energies,  $E_\nu = 3$  GeV (left panel) and  $E_\nu = 10$  GeV (right panel). It can be observed from the figures that as one moves to the higher  $\nu$  and  $Q^2$  regions, the deep inelastic scattering becomes the dominant process in the neutrino interactions, where the (anti)neutrino interacts with the quarks and gluonic degrees of freedom in the nucleons [19]. The deep inelastic scattering process, in this kinematic region, is described using perturbative quantum chromodynamics (QCD). However, there is currently no sharp kinematic boundary on  $\nu$  and  $Q^2$  for the onset of deep inelastic scattering in the literature. Generally,  $Q^2 > 1$  GeV<sup>2</sup> is chosen for the onset of deep inelastic scattering. A kinematic constraint of  $W > 2$  GeV is also applied to safely describe the deep inelastic scattering region. However, in the kinematic region of  $Q^2 < 1$  GeV<sup>2</sup>, nonperturbative QCD effects must be taken into serious consideration. In this region, which is also known as the transition region, it is expected that the prin-

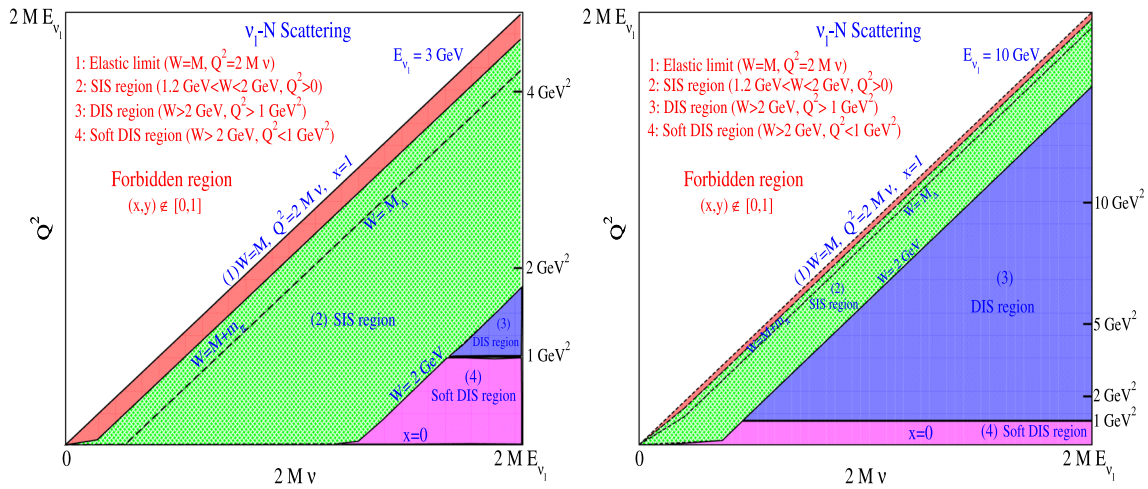


**Fig. 1** Allowed kinematic region for  $\nu_l - N$ ; ( $l = \mu$ ) scattering in the  $(Q^2, \nu)$  plane for  $E_\nu = 3 \text{ GeV}$  (left panel) and  $E_\nu = 10 \text{ GeV}$  (right panel) for  $Q^2 \geq 0$  ( $Q^2$  is the four-momentum transfer squared). Invariant mass square is defined as  $W^2 = M^2 + 2M\nu - Q^2$  and the elastic limit is  $x = \frac{Q^2}{2M\nu} = 1$ . The forbidden region in terms of  $x$  and  $y = \frac{\nu}{E_\nu} = \frac{(E_\nu - E_l)}{E_\nu}$  is defined as  $x, y \notin [0, 1]$ . Processes like photon emission are possible in the extreme left band (the region between  $W = M$  and  $W < M + m_\pi$ ). The SIS region

is defined as the region for which  $M + m_\pi \leq W \leq 2 \text{ GeV}$  and  $Q^2 \geq 0$ , the deep inelastic scattering region is defined as the region for which  $Q^2 \geq 1 \text{ GeV}^2$  and  $W \geq 2 \text{ GeV}$ , and the soft deep inelastic scattering region is defined as  $Q^2 < 1 \text{ GeV}^2$  and  $W \geq 2 \text{ GeV}$ . The soft deep inelastic scattering region is also nothing but the SIS region. The extreme left band also gets the contribution for the bound nucleons in nuclear targets through  $np - nh$  like  $2p$ - $2h$  excitations. The boundaries between regions are not sharply established and are suggestive only

ciple of quark-hadron duality can be used to obtain the neutrino cross sections. However, little work has been undertaken either theoretically or experimentally to understand the neutrino cross section using quark-hadron duality. This issue was raised recently in the Snowmass [20] and NUSTEC [21] meetings.

In Fig. 2, we show the relative importance of the above processes (quasielastic, inelastic and deep inelastic scattering) through the energy dependence of their cross sections [22]. This figure depicts the total scattering cross section per nucleon per unit energy of the incoming particles versus neutrino (left panel) and antineutrino (right panel) energy in the charged current-induced process. The dashed, dashed-dotted, and dotted lines represent the contributions from the quasielastic scattering, inelastic resonance (RES), and deep inelastic scattering processes, respectively. The sum of all the scattering cross sections (TOTAL) is shown by the solid line [22]. The experimental results include the data from older experiments (ANL and BNL) as well as experiments performed recently using the (anti)neutrino beam. It can be observed that the experimental error bars are large and that precise measurements are needed. In all the present-generation neutrino experiments, nuclear targets such as  $^{12}\text{C}$ ,  $^{16}\text{O}$ ,  $^{40}\text{Ar}$ ,  $^{56}\text{Fe}$ , and  $^{208}\text{Pb}$ , are being used, and the interactions take place with the nucleons that are bound inside the nucleus, where nuclear medium effects (NME) become important.

These neutrino experiments measure (anti)neutrino events that are a convolution of the

- (i) energy-dependent neutrino flux and
- (ii) energy-dependent neutrino-nucleon cross section.

Therefore, an understanding of the energy dependence of the neutrino-nucleon cross sections is highly desirable. In the context of the present neutrino oscillation experiments using nuclear targets, understanding the energy dependence of the NME is of great importance. Especially in the precision era of neutrino oscillation experiments, to achieve accuracy of a few percent (2–3%) in the systematics, a good understanding of neutrino-nucleon and neutrino-nucleus cross sections is required. At present, due to the lack of understanding of these cross sections, an uncertainty of 25–30% in the systematics arises. The study of neutrino interactions with matter is important not only for understanding the neutrino physics, but also to gain greater insight into hadronic interactions in the weak sector, where there is an additional contribution of axial vector current besides the vector current.

In the case of the quasielastic process, the general consideration of the NME includes the Fermi motion, Pauli blocking, and the multinucleon correlation effects. In the case of single pion production, one considers Fermi motion and Pauli blocking of the nucleon as well as the modification of the properties of the various excited resonances, especially their masses and widths, in the medium. However, these modifications are well studied only in the case of  $\Delta$  resonance. In addition, the pion produced in the decay of these resonances undergoes final state interactions with the residual nucleus, where charge exchange processes (e.g.

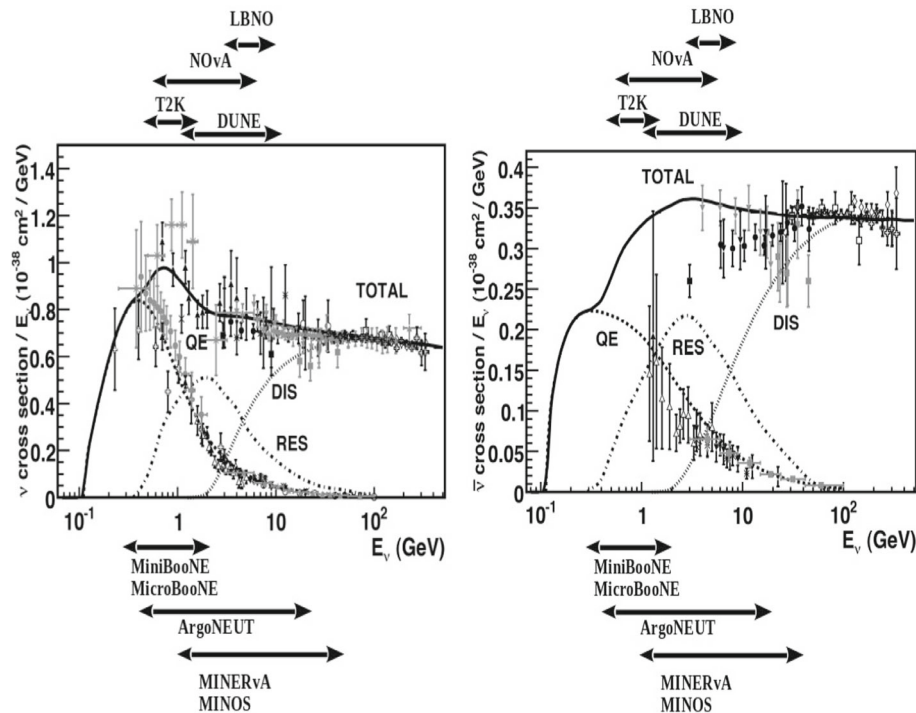


**Fig. 2** Charged current-induced total scattering cross section per nucleon per unit energy of the incoming particles vs. neutrino (left panel) and antineutrino (right panel) energy for all three processes labeled on the curve along with the total scattering cross sections. Dashed line shows the contribution from the quasielastic scattering, while the dashed-

dotted and dotted lines represent the contributions from the inelastic resonance (RES) and deep inelastic scattering, respectively. The sum of all the scattering cross sections (TOTAL) is shown by the solid line [22]. We have also mentioned the energy region of various experiments

$\pi^- p \rightarrow \pi^0 n$ ) or modulation in its energy and momentum or pion absorption ( $\pi NN \rightarrow NN$ ) may take place. If the produced pion is absorbed, it mimics a quasilike event. In the case of deep inelastic scattering, shadowing and antishadowing corrections become important in the region of low  $x$ , the Bjorken variable. In the intermediate region of  $x$ , the mesonic contributions become important, where the interaction of an intermediate vector boson ( $W, Z$ ) takes place with the virtual mesons in the nucleus, and in the region of high  $x$ , Fermi motion effects are important.

The consideration of different NME is model-dependent, and there is no consensus with regard to any particular nuclear model [23, 24]. In order to understand the NME in (anti)neutrino-nucleus scattering, additional data with greater precision are needed.

This volume is devoted to the study of neutrino interactions from the nucleons and nuclei in the region of intermediate and high energies, and comprises 17 articles discussing quasielastic, single pion production, other inelastic processes, and the deep inelastic scattering of (anti)neutrinos from the nucleons and nuclei. All the contributing articles are arranged according to the following aspects of their content:

- (i) Experimental
- (ii) Theoretical
- (iii) Phenomenological.

To enable a general historical understanding of neutrino experiments from Gargamelle to Main Injector Neutrino Experiment to study  $\nu - A$  interactions (MINERvA), a bird's-eye view is lucidly illustrated by Morfin [25], where he summarizes various attempts made to explore the structure of the nucleon with neutrinos. In the next five articles, the current status and results of some important experiments being performed in the few-giga-electron-volt energy region are discussed, including the efforts of MINERvA, NOvA, Micro Booster Neutrino Experiment (MicroBooNE), Argon Neutrino Teststand (ArgoNeuT), and neutrino interaction physics in neutrino telescopes. The MINERvA experiment at Fermilab took data using the (anti)neutrinos at the Main Injector (NuMI) beamline from 2009 to 2019 in the low-energy and medium-energy range that peak at 3 GeV and 6 GeV, respectively, using several nuclear targets including carbon in scintillators, oxygen in water, and iron and lead, in order to understand the NME in a wide range of Bjorken  $x$  and  $Q^2$ . Lu et al. [26], on behalf of the MINERvA collaboration, present the latest results of the differential and total scattering cross sections for the inclusive, quasielastic, inelastic single pion, and single kaon processes, among others, and highlight their salient observations. The NOvA at Fermilab has been collecting data in the NuMI neutrino beam since 2014, and the expectation is that it will continue until 2026. Shanahan and Vahle [27], on

behalf of the NOvA collaboration, present experimental results in three neutrino flavor oscillation scenarios as well as the results of the differential scattering cross sections for the inclusive channel and for the coherent pion production processes. The MicroBooNE and ArgoNeUT Liquid Argon Time Projection Chambers (LArTPC) at Fermilab have collected data in the NuMI and Booster Neutrino Beams, respectively. The neutrino interaction measurements of these experiments are presented by Duffy et al. [28] for the charged-current  $\nu_\mu$  scattering in the inclusive channel,  $0\pi$  channel (in which no pions but some number of protons may be produced), and for single pion production (including production of both charged and neutral pions), as well as measurements of inclusive scattering cross sections for  $\nu_e + \bar{\nu}_e$  interactions. Katori et al. [29] discuss neutrino interaction physics in neutrino telescopes, where interactions are detected via Cherenkov radiation emitted by the charged secondaries, and specifically discuss in detail the largest neutrino telescope in operation to date, the IceCube Neutrino Observatory.

These articles are followed by ten articles dealing with various aspects of theoretical developments in the elastic, quasielastic, inelastic, and deep inelastic scattering of (anti)neutrinos from nucleons and nuclei. Benhar [30] elucidates the problems and uncertainties in evaluating the cross sections with NME and also deals with the theoretical understanding required to unravel the flux-averaged neutrino-nucleus cross section by discussing in detail quasielastic scattering, single pion production and, very briefly, deep inelastic scattering processes. Nuclear model dependence in quasielastic scattering is discussed by Amaro et al. [31], where they explicitly describe the neutrino-nucleus scattering cross section using a superscaling (SuSA) approach by considering one- and two-body currents, showing first that the model explains well the electron scattering data and then by applying it to understand weak interaction-induced processes. Jackowicz and Nikolakopoulos [32] have studied the NME in quasielastic neutrino-nucleus scattering using nuclear mean field and random phase approximation, and highlight the differences between neutrino- and antineutrino-induced reactions. Chanfray et al. [33] describe the neutrino-nucleus scattering cross section for a CCQE process using response functions and spectral functions, and highlight the dependence of multinucleon correlation effects in the different models. Alvarez-Ruso et al. [34] discuss neutrino interactions with matter, with a particular emphasis on the MiniBooNE anomaly. Fatima et al. [35] highlight the importance of  $\bar{\nu}_\mu$ -induced quasielastic production of hyperons leading to pions (the reaction which is forbidden for neutrino-induced processes due to the  $\Delta S = \Delta Q$  rule). The effects of the second class currents in the axial vector sector with and without T-invariance are discussed, as well as the effect of SU(3) symmetry breaking. Paschos [36] discusses a model for the flavor-changing neutral current of leptons.

Neutrino-nucleon reactions in the resonance region have been studied by Sato [37] using a dynamical coupled channel (DCC) model by restoring full unitarity.

The cross sections of charged current neutrino reaction are examined to analyze the mechanism of the neutrino-induced meson production reaction, and a possible way to test the model of the axial vector current contribution. In the case of deep inelastic scattering, the evolution of the electroweak structure functions of nucleons has been studied by Reno [38] in the context of muon and tau neutrino and antineutrino scattering. Ansari et al. [39], in their review article, discuss the effect of nonperturbative corrections such as target mass correction and higher twist effects, perturbative evolution of the parton densities, nuclear medium modifications of the nucleon structure functions, and nuclear isoscalar corrections on the weak nuclear structure functions in (anti)neutrino-nucleus scattering in the deep inelastic scattering region. The numerical results for the structure functions and the cross sections are compared with some of the available experimental data including the recent results from MINERvA. The predictions are made in an argon nuclear target which is planned to be used as a target material in Deep Underground Neutrino Observatory (DUNE) at the Fermilab.

Monte Carlo (MC) neutrino event generators play an important role in the design, optimization, and execution of neutrino oscillation experiments, and the two most widely used neutrino event generators in the present experimental physics community are GENIE and NEUT, which predict the neutrino event rates using various inputs including the (anti)neutrino-nucleus scattering cross sections and the final state interactions of the produced hadrons in the nucleus. In this volume, the main features of these two generators are elaborated individually. GENIE, as explained by Alvarez-Ruso et al. [40], with its gradual evolution and adaptability, is assumed to become a standard tool, forming an indispensable part of many experiments, and has been widely tested against neutrino cross-sectional data. Important features of the NEUT MC generator are illustrated by Hayato et al. [41]. It can be used to simulate interactions for neutrinos between 100 MeV and a few tera-electron-volts of energy, and is also capable of simulating hadron interactions within a nucleus.

We are thankful to all the authors who have contributed to this volume. Their efforts are truly commendable, and we hope that this volume will be helpful to students and both young and senior researchers in the field of neutrino physics, and will stimulate new ideas and investigation. Special thanks are due to B. Ananthanarayan, member of the editorial board of EPJ-ST, who invited us to present this topical volume. The help and cooperation of the editorial team of EPJ-ST is duly acknowledged.

## References

1. W. Pauli, Letter to L. Meitner and her colleagues dated 4 December 1930 (letter open to the participants of the conference in Tübingen) (1930), recorded in W. Pauli, Wissenschaftlicher Briefwechsel mit Bohr, Ein-

- stein, Heisenberg u.a., Band 11 (Springer, Berlin, 1985) p. 39. A reference to ‘neutrino’ is seen in a letter from Heisenberg to Pauli on 1 December 1930: ‘Zu Deinen Neutronen möchte ich noch bemerken: ...’
2. E. Fermi, *Nuovo Cimento* **11**, 157 (1934)
  3. C.-S. Wu, E. Ambler, R.W. Hayward, D.D. Hoppes, R.P. Hudson, Experimental test of parity conservation in beta decay. *Phys. Rev.* **105**(4), 1413 (1957)
  4. M. Goldhaber, L. Grodzins, A.W. Sunyar, Helicity of neutrinos. *Phys. Rev.* **109**(1958), 1015 (1958)
  5. R.E. Marshak, E.C.G. Sudarshan, *Proc. Int. Conf. Elem. Part*, Padua (1957)
  6. R.E. Marshak, E.C.G. Sudarshan, *Phys. Rev.* **109**, 1860 (1958)
  7. A. Salam, *Nuovo Cimento* **5**, 299 (1957)
  8. R.P. Feynman, M. Gell-Mann, *Phys. Rev.* **109**, 193 (1958)
  9. J.J. Sakurai, *IL Nuovo Cimento* **VII**, 649 (1958)
  10. F. Reines, C.L. Cowan, *Nature* **178**(4531), 446–449 (1956)
  11. F. Reines, C.L. Cowan Jr., *Phys. Rev.* **113**, 273 (1959)
  12. S.L. Glashow, *Nucl. Phys.* **22**, 579 (1961)
  13. S. Weinberg, *Phys. Rev. Lett.* **19**, 1264 (1967)
  14. A. Salam, *Conf. Proc. C* **680519**, 367 (1968)
  15. S. Mele, *Adv. Ser. Direct. High Energy Phys.* **23**, 89 (2015)
  16. M. Sajjad Athar, S.K. Singh, *The Physics of Neutrino Interactions* (Cambridge University Press, 2020). <https://doi.org/10.1017/9781108489065.029>
  17. B. Pontecorvo, *Sov. Phys. JETP* **7**, 172 (1958)
  18. Z. Maki, M. Nakagawa, S. Sakata, *Prog. Theor. Phys.* **28**, 870 (1962)
  19. M. Sajjad Athar, J.G. Morfin, *J. Phys. G* **48**, 034001 (2021)
  20. Snowmass workshop on ‘Theoretical tools for neutrino scattering: the interplay between lattice QCD, EFTs, nuclear physics, phenomenology, and neutrino event generators’, 23–25 August, 2021. <https://indico.fnal.gov/event/50335/overview>
  21. C. Andreopoulos et al. [NuSTEC], Summary of the NuSTEC Workshop on Shallow- and Deep-Inelastic Scattering. [arXiv:1907.13252](https://arxiv.org/abs/1907.13252) [hep-ph]
  22. P. Lipari, L. Maurizio, S. Francesca, *Phys. Rev. Lett.* **74**, 4384 (1995)
  23. L. Alvarez-Ruso et al., NuSTEC White Paper: status and challenges of neutrino-nucleus scattering. *Prog. Part. Nucl. Phys.* **100**, 1 (2018)
  24. T. Katori, M. Martini, *J. Phys. G* **45**, 013001 (2018)
  25. J.G. Morfin, From Gargamelle to MINERvA: exploring the structure of the nucleon with neutrinos. *Eur. Phys. J. Spec. Top.* (2021). <https://doi.org/10.1140/epjs/s11734-021-00298-4>
  26. X.-G. Lu et al., Exploring neutrino-nucleus interactions in the GeV regime using MINERvA. *Eur. Phys. J. Spec. Top.* (2021). <https://doi.org/10.1140/epjs/s11734-021-00296-6>
  27. P. Shanahan, P. Vahle, Physics with NOvA—a half-time review. *Eur. Phys. J. Spec. Top.* (2021). <https://doi.org/10.1140/epjs/s11734-021-00285-9>
  28. K. Duffy et al., Neutrino interaction measurements with the MicroBooNE and ArgoNeuT liquid argon time projection chambers. *Eur. Phys. J. Spec. Top.* (2021). <https://doi.org/10.1140/epjs/s11734-021-00297-5>
  29. T. Katori, J.P. Yanez, T. Yuan, Neutrino interaction physics in neutrino telescopes. *Eur. Phys. J. Spec. Top.* (2021). <https://doi.org/10.1140/epjs/s11734-021-00292-w>
  30. O. Benhar, Unraveling the flux-averaged neutrino-nucleus cross section. *Eur. Phys. J. Spec. Top.* (2021). <https://doi.org/10.1140/epjs/s11734-021-00290-y>
  31. J.E. Amaro et al., Neutrino-nucleus scattering in the SuSA model. *Eur. Phys. J. Spec. Top.* (2021). <https://doi.org/10.1140/epjs/s11734-021-00289-5>
  32. N. Jachowicz, A. Nikolakopoulos, Nuclear medium effects in neutrino- and antineutrino-nucleus scattering. *Eur. Phys. J. Spec. Top.* (2021). <https://doi.org/10.1140/epjs/s11734-021-00286-8>
  33. G. Chanfray, M. Ericson, M. Martini, Multinucleon excitations in neutrino-nucleus scattering: connecting different microscopic models for the correlations. *Eur. Phys. J. Spec. Top.* (2021). <https://doi.org/10.1140/epjs/s11734-021-00291-x>
  34. L. Alvarez-Ruso, E. Saul-Sala, Neutrino interactions with matter and the MiniBooNE anomaly. *Eur. Phys. J. Spec. Top.* (2021). <https://doi.org/10.1140/epjs/s11734-021-00293-9>
  35. A. Fatima, M. Sajjad Athar, S.K. Singh,  $\bar{\nu}_\mu$  induced quasielastic production of hyperons leading to pions. *Eur. Phys. J. Spec. Top.* (2021). <https://doi.org/10.1140/epjs/s11734-021-00272-0>
  36. E.A. Paschos, Flavor changing neutral couplings for leptons. *Eur. Phys. J. Spec. Top.* (2021). <https://doi.org/10.1140/epjs/s11734-021-00294-8>
  37. T. Sato, Neutrino-nucleon reactions in resonance region. *Eur. Phys. J. Spec. Top.* (2021). <https://doi.org/10.1140/epjs/s11734-021-00284-w>
  38. Mary Hall Reno, Evolution of the electroweak structure functions of nucleons. *Eur. Phys. J. Spec. Top.* (2021). <https://doi.org/10.1140/epjs/s11734-021-00288-6>
  39. V. Ansari et al., Deep inelastic (anti)neutrino-nucleus scattering. *Eur. Phys. J. Spec. Top.* (2021). <https://doi.org/10.1140/epjs/s11734-021-00277-9>
  40. L. Alvarez-Ruso et al., Recent highlights from GENIE v3. *Eur. Phys. J. Spec. Top.* (2021). <https://doi.org/10.1140/epjs/s11734-021-00295-7>
  41. Y. Hayato, L. Pickering, The NEUT Neutrino Interaction Simulation Program Library. *Eur. Phys. J. Spec. Top.* (2021). <https://doi.org/10.1140/epjs/s11734-021-00287-7>